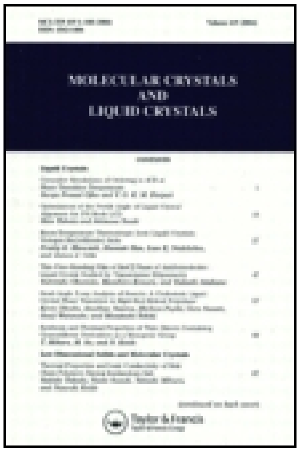

Molecular Crystals and Liquid Crystals Science and Technology. Section A. Molecular Crystals and Liquid Crystals

Publication details, including instructions for authors and subscription information:
http://www.tandfonline.com/loi/gmcl19

Phenomenological Scattering Models for Nematic Droplet/Polymer Films: Refractive Index and Droplet Correlation Effects

Paul S. Drzaic [a] & Anne M. Gonzales [a]

[a] Raychem Corporation, 300 Constitution Drive, Menlo Park, CA, 94025, USA

Version of record first published: 04 Oct 2006.

To cite this article: Paul S. Drzaic & Anne M. Gonzales (1992): Phenomenological Scattering Models for Nematic Droplet/Polymer Films: Refractive Index and Droplet Correlation Effects, Molecular Crystals and Liquid Crystals Science and Technology. Section A. Molecular Crystals and Liquid Crystals, 222:1, 11-20

To link to this article: http://dx.doi.org/10.1080/15421409208048676

Mol. Cryst. Liq. Cryst. 1992, Vol. 222, pp. 11–20
Reprints available directly from the publisher
Photocopying permitted by license only

Printed in the United States of America

Phenomenological Scattering Models for Nematic Droplet/Polymer Films: Refractive Index and Droplet Correlation Effects

Paul S. Drzaic and Anne M. Gonzales

Raychem Corporation, 300 Constitution Drive, Menlo Park CA 94025 USA

(Received October 2, 1991)

Abstract

We establish some phenomenological relationships for the scattering properties of select films of nematic dispersions. For powered films of similar structure but containing different LC's, angle and polarization-dependent transmission measurements show that film scattering depends simply on the refractive index mismatch between the polymer and nematic. We find little wavelength dependence on the film scattering cross section when the refractive index mismatch between LC and polymer is small. We examine the importance of the refractive index gradient produced by anti-correlated LC droplets as a factor in the film scattering of unpowered films. We find that in unpowered films it appears that these gradients are at least as important in contributing to film scattering as the more familiar LC/polymer refractive index gradient.

Introduction

Nematic dispersions[1-3] (known as NCAP or PDLC, among others) possess electrically-controllable scattering properties, changing from a translucent to a transparent state upon application of an electric field. The scattering properties of nematic dispersions are arguably the most important aspects of these materials, with applications of these films making either direct or indirect use of these scattering properties.

A number of groups have addressed the theoretical and experimental aspects of light scattering from nematic droplets. The choice of the most appropriate theoretical model depends on the magnitude of kR ($k = 2\pi n/\lambda$, R=droplet radius). For kR<<1, Rayleigh-Gans[4] treatments have been used to model film scattering. Reasonable agreement between experiment and theory has been found for dilute films of submicron droplets.[5,6] For larger kR, anomalous diffraction,[7] ray tracing,[8] and Mie[9] theories have been applied to describe the scattering properties of individual droplets.

These theoretical treatments, while describing fundamental scattering processes, have been difficult to apply to many types of films of practical interest. NCAP films with droplet sizes of several microns (kR> 50) form interesting devices. The volume fraction of liquid crystal (LC) in many films can range from 0.4 to 0.9, making multiple scattering important. Additionally, in many films the thickness of the polymer layer separating neighboring droplets is on the same size scale of the wavelength of light. In this case the refractive index of neighboring droplets, as well as the polymer matrix, will probably affect the light scattering of a droplet. These factors make it difficult to apply fundamental light scattering theories to predict *a priori* film scattering profiles.

In this paper, we report some early results in a study of the light scattering properties of a select set of NCAP films. The NCAP films studied here are characterized for both structure and optical properties. We measure the transmission properties of films as a function of light polarization, its incident angle, and LC properties. These data are used to establish empirical relationships between these properties and the light scattering properties of film. We find that the scattering properties of powered films are defined by the refractive index (RI) properties of the nematic in a way that is consistent between different films. By comparing select powered and unpowered films, we are able to probe the contribution to film scattering of LC/LC RI gradients, as well as from LC/polymer RI gradients. We find that RI gradients across LC/polymer interfaces and between correlated LC droplets are both important in determining the scattering properties of the film.

Experimental

Films of nematic dispersions were constructed by the emulsification method,[2] using PVA (Airvol 205, Air Products) as the matrix polymer (polymer:LC weight ratio 2:3). Mean volume diameters for the emulsions were measured for each material before coating (Multisizer, Coulter Industries). Film substrates were ITO-coated glass and ITO-coated polyethersulfone (Southwall Technologies).

Table 1. Refractive index values for components of NCAP films (20 C).

	PVA	ZLI 1840		ZLI 3219		E49	
		$n_\perp$	$n_\parallel$	$n_\perp$	$n_\parallel$	$n_\perp$	$n_\parallel$
450 nm	1.5108	1.5085	1.6678	1.5268	1.7680	1.5527	1.8637
550 nm	1.5106	1.4968	1.6430	1.5168	1.7278	1.5345	1.8063
650 nm	1.5106	1.4901	1.6287	1.5110	1.7047	1.5240	1.7734

Transmission measurements were performed using either a 5 mW HeNe laser, or a collimated beam from a 50 W xenon arc lamp, using 10 nm bandwidth filters to select the wavelength. Scattered light was collected using f/12 optics (defined as the ratio of the distance between the film and detector to the diameter of the photodiode). Polarization of the collimated beam, when employed, was chosen to be parallel or perpendicular to the rotation axis of the sample. For the angle-dependent measurements, the film was rotated through an angle θ, with the light source and detector fixed in space. Transmission values at each θ were corrected for reflection losses by dividing by the transmission of a film blank. This blank consisted of the same ITO-coated glass and PES substrates as before, but bonded together with a transparent polymer (PVA). Table 1 lists the wavelength-dependent refractive indices of the polymer and nematics. PVA RI values were measured with an Abbe refractometer. Liquid crystal RI values were obtained from E. Merck (Darmstadt).

Film construction and light scattering mechanisms

The construction of the nematic dispersions discussed here is important in understanding the light scattering data collected. Electron micrographs[10] of films using a PVA binder at a liquid crystal:polymer ratio of 3:2 show that the nematic exists predominantly within spheroidal cavities in the film. Due to anisotropic shrinkage of the polymer during the film formation, the spheroidal cavities are oblate in shape, with the major axes of the spheroid lying predominantly within the film plane.

The nematic director in these films adopts a bipolar[2] configuration. Figure 1 shows schematically how the nematic is aligned within unpowered and powered films. In unpowered films, the director symmetry axis for each droplet is oriented randomly within the film plane, with no interdroplet correlation.[11] At high fields, however, the nematic symmetry axis of each droplet is aligned with the field.

The RI of the droplet will be polarization and direction dependent. It is useful to define an effective RI (n_{eff}) for the droplet,[12] derived simply from the angle-dependent radius of the RI ellipsoid.[13] We define the RI mismatch of the droplet and matrix as n_{mis} (Equation 1). Equation (1) includes a Snell's Law correction for refraction of light

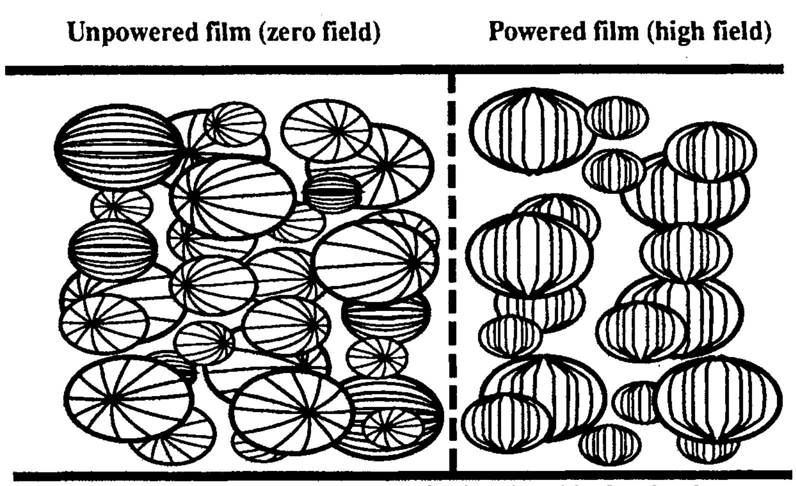

Figure 1. Schematic of director fields of spheroidal bipolar droplets at zero and at high fields.

traveling from air into the polymer.

$$n_{mis} = n_{ef} - n_{pol} = \frac{n_{\perp}}{\sqrt{1 - \left(\frac{\sin[\theta_{air}]}{n_{pol}}\right)^2 \left(1 - \left[\frac{n_{\perp}}{n_{\parallel}}\right]^2\right)}} - n_{pol} \tag{1}$$

It is well known that the scattering properties of NCAP/PDLC films are derived from a spatially-varying RI within the film. The most obvious source of this index variation is the difference between the RI values of the nematic and the polymer. The difference between the extraordinary index of the LC ($n_{\parallel}$) and the polymer RI (n_{pol}) is usually substantial, while the ordinary RI of the LC ($n_{\perp}$) is typically close in magnitude to n_{pol}. Given these conditions, only one polarization of light incident on a droplet (the one aligned with $n_{\parallel}$) is scattered significantly by the polymer/LC RI gradient.

A second source of RI gradients arises from the uncorrelated symmetry axes of neighboring droplets in a film. The polymer boundary separating droplets is often on the order of a few hundred nanometers, so that two neighboring droplets can be expected to generate a RI gradient that is significant on the size scale of light. A substantial RI gradient (equal to Δn) can occur for two droplets with perpendicularly-aligned symmetry axes (anti-correlated droplets). Alternatively, droplets with similar orientation directions will produce no RI gradient. The contribution of these RI gradients to film scattering for a volume of film will be integrated over paired orientations of neighboring droplets. Note that these LC/LC gradients will be absent in powered films, since all droplets in this case are aligned in a common direction (Figure 1).

A third source of a RI gradient is the spatially-varying director field at the curved surfaces of the cavity walls. Calculations[4] of the nematic alignment within cavities indicate that RI gradients in bipolar droplets will occur in optically thin layers near the cavity walls. We expect that the coupling of this gradient to the optical field will be weak, and that this mechanism will not be important here.

To date, no experimental evidence has been reported which helps distinguish between these various mechanisms. In the following sections, we examine select films to illuminate the importance of these different mechanisms.

Polarization and angle-dependent scattering of powered films

From equation 1, we see that the LC/polymer RI mismatch in powered films will depend on the angle of incidence of the light. To determine the importance of this LC/polymer mismatch, we constructed a series of films with nearly-identical morphology, but employing different LC's. For this study, ZLI-1840, ZLI-3219, and E49 were emulsified to a volume-weighted mean diameter of 3.25 ±0.03 μm. Each film was coated to a

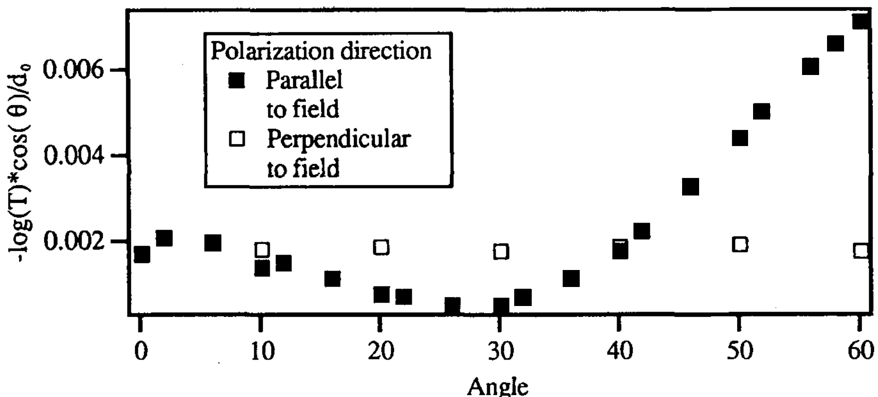

Figure 2. Angle-dependent scattering of ZLI 1840 at 550 nm, f/12 optics. Data plotted as absorbance [−log(T)], corrected for angle-dependent path length.

thickness between 13.6 and 16.9 μm. We measured the polarization-dependent transmission (f/12 optics) of each film from 0°-60°, using 450 nm, 550 nm, and 650 nm light.

For a collection of dilute scattering centers, the transmission will typically drop exponentially with sample thickness.[14] At non-zero angles, the path length through the film increases by $1/\cos\theta$. To correct for this path length with angle, each transmission T at angle θ was transformed into a corrected absorbance $A_{cor} = -\log[T]\cos(\theta)/d$, where d is the film thickness at 0°. This thickness correction will become less accurate as the magnitude of film scattering increases. With strong scattering, some scattered light is scattered back into the original ray direction, so that the transmission drops off more weakly with increasing thickness. We expect that any errors caused by this path length correction in highly-scattering films will not be large enough to change any of the conclusions drawn in this study.

Figure 2 shows the angle and polarization-dependent A_{cor} of ZLI-1840 at 550 nm. For light polarized parallel to the plane of incidence, the corrected absorbance is strongly angle dependent. For the perpendicular polarization, the transmission is independent of incident angle. This behavior is similar to that observed in previous studies of films constructed using phase separation methods.[12,15]

In our model, the highest transmission values should occur when the RI mismatch n_{mis} is a minimum. Figure 3 shows a plot of A_{cor} vs. n_{mis} for the ZLI 1840 film; n_{mis} is calculated using Equation (1) and the values in Table (1). Since $n_{\perp} < n_{pol}$ for this system, n_{mis} will be minimized at an angle $\theta > 0°$. We see that each curve shows a minimum in A_{cor} at $\theta > 0°$, as expected. The minimum for 550 nm light is near $n_{mis} = 0.000$. The minima for 450 nm and 650 nm light, however, appear at 0.006 and −0.007. These values are outside the ±0.004 uncertainty in n_{mis} expected for these measurements, based on

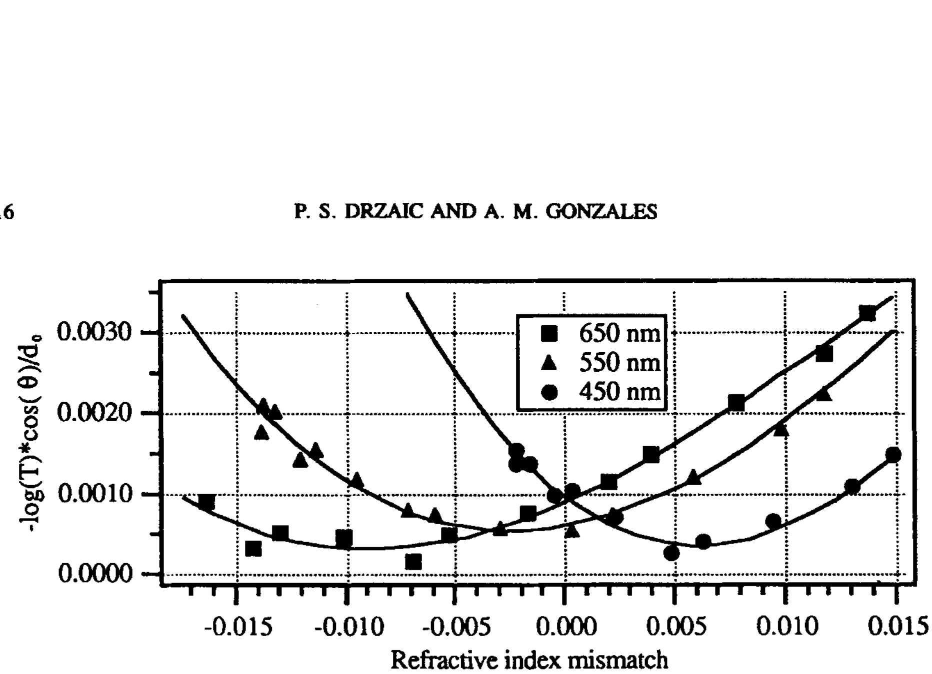

Figure 3. Corrected absorbance of ZLI 1840 at 450, 550, and 650 nm, plotted vs. refractive index mismatch between LC and polymer.

uncertainties in the RI values and measurement angles. While at this stage we cannot completely rule out some systematic error in the measurements, this disagreement may also indicate that the RI values of the polymer or LC have changed from their values in the bulk. Measurements of the RI of PVA placed in contact with the liquid crystals used here show little change in the PVA RI. It is possible, however, that the composition of the ZLI 1840 has changed slightly during sample preparation.

Figure 4 shows composite plots of for the three different LC films, at each of the three wavelengths. The most striking feature of these plots is that the correlation of A_{cor} with n_{mis} across the three films, despite the large differences in birefringence between the different nematic mixtures. These data clearly show that the scattering properties of powered NCAP films at these cavity sizes are completely determined by the RI mismatch between polymer and LC.

Figure 5 compares the wavelength-dependent scattering for the ZLI 3219 films. Interestingly, there is little wavelength dependence of the scattering for n_{mis} <0.04. Only for n_{mis}> 0.04 is there a clear wavelength dependence of the scattering. The data for ZLI 1840 and E49 films show similar behavior, in that for equal n_{mis}, different wavelengths show approximately the same scattering level for n_{mis} <0.04.

The wavelength dependency of the scattering cross section is one of the primary differences between different models of light scattering for nematic droplets. The strongest wavelength dependence is predicted by Rayleigh-Gans theory,[4] with the scattering cross section σ scaling as $1/\lambda^4$. Since a key assumption for that theory is kR<<1, it is not surprising that this strong dependence on wavelength is not seen. At the other extreme, a ray-

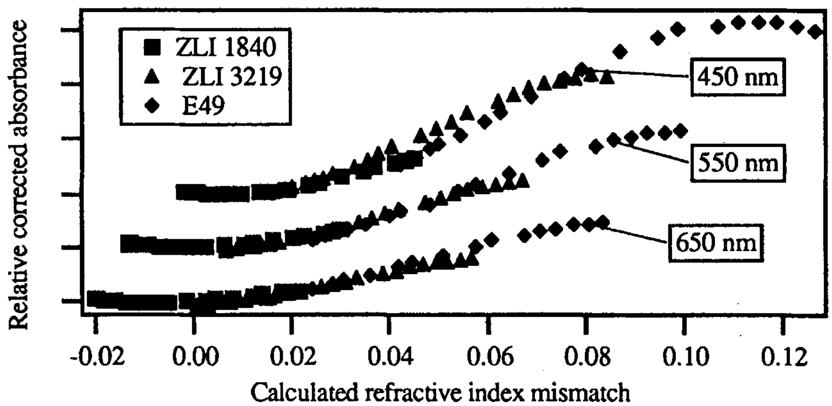

Figure 4. Corrected absorbance vs. calculated refractive index mismatch for NCAP films. The three wavelength sets are offset vertically for clarity.

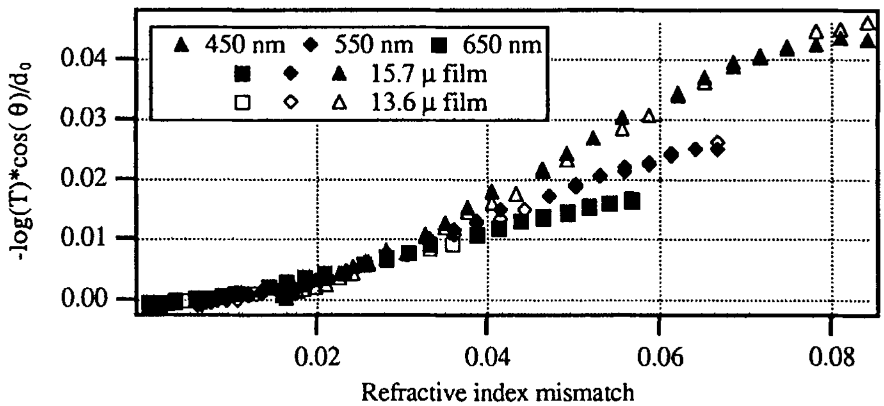

Figure 5. Corrected absorbance vs. calculated refractive index mismatch for ZLI 3219 NCAP films. There is little wavelength dependence of scattering for $n_{mis} < 0.04$. Also note that the data from the two different film thicknesses superimposes well, supporting the cos(θ)/d correction used in analyzing the data.

tracing approach (based on refraction through a birefringent sphere) predicts no intrinsic wavelength dependence of the scattering.[8] The wavelength dependence observed at large n_{mis} argues against this model being the dominant mechanism for the scattering properties observed here.

The anomalous diffraction (AD) approach outlined by Žumer[7] and the Mie calculations of Nomura *et. al.*[9] do not predict strong wavelength dependencies for the droplet sizes used here. The AD model predicts a $1/\lambda^2$ dependence on scattering for kR near 1, and a cross section that oscillates around a central value with further increase in kR. The Mie calculations show strongly varying wavelength dependencies on droplet size. In the films studied here, the broad distribution of droplet sizes (kR ranging from 20 to 80) will smear out any oscillation in scattering cross section.

We expect that future, more extensive work will better determine the wavelength dependence of scattering in these systems. The onset of a wavelength dependence for scattering may be helpful in placing limits on the applicability of these theories to various film systems.

LC/polymer vs. LC/LC refractive index gradients

In the systems discussed so far, the high fields (> 6 V/μm) applied guarantee a uniform alignment of the nematic within the film. We expect little contribution to the film scattering from LC/LC gradients, since the director fields in a powered film are highly correlated with each other. The angle-dependent cross section data shows the magnitude of scattering observed from LC/polymer RI gradients. In contrast, unpowered film scattering will possess contributions from both LC/LC and LC/polymer RI gradients.

The differences in alignment between powered and unpowered films will change the relative efficiency of scattering from LC/polymer gradients. In powered films probed with light <u>polarized along the nematic alignment direction</u>, all the incident light will be scattered by the large RI gradient $n_{\|} - n_{pol}$. In contrast, in unpowered films the RI gradients will vary between $n_{\|} - n_{pol}$ and the much smaller $n_{\perp} - n_{pol}$, so that some of the incident light will be scattered only weakly by the small RI gradient. Thus, we expect *a priori* that LC/polymer scattering will be approximately twice as efficient per unit thickness for powered films probed with the proper light polarization as it will for unpowered films.

The set of films described in previous section can be used to determine qualitatively the relative importance of LC/LC RI gradients, compared to LC/polymer RI gradients. In the ZLI 1840 system, the RI mismatch in unpowered films (equivalent to $\theta=0°$) is similar in magnitude to the RI mismatch in E49 at high angles. Figure 6 shows a logarithmic plot of transmission (<u>not</u> corrected for thickness or angle, but still corrected for reflection losses) for powered E49 films at 450 nm, and for unpowered ZLI 1840 films at all three wavelengths. It is apparent that the transmission values are approximately equal for n_{mis} near 0.12. However, based on our previous discussion, the transmission values should <u>not</u> be equal if LC/polymer scattering is dominant. First, the E49 data points were taken over the angular range $50° < \theta < 60°$. With the $1/\cos(\theta)$ dependence of thickness, the effective path length through the film is 27-32 μm. The path length through the ZLI 1840 film at 0°, in comparison, is only 17 μm. Due to this path length difference, the E49 films should possess twice the scattering power of the ZLI 1840 film. Second, the highly correlated nature of the droplets in the powered E49 film should make it more efficient at scattering than the ZLI 1840 by another factor of two (as described in the previous paragraph).

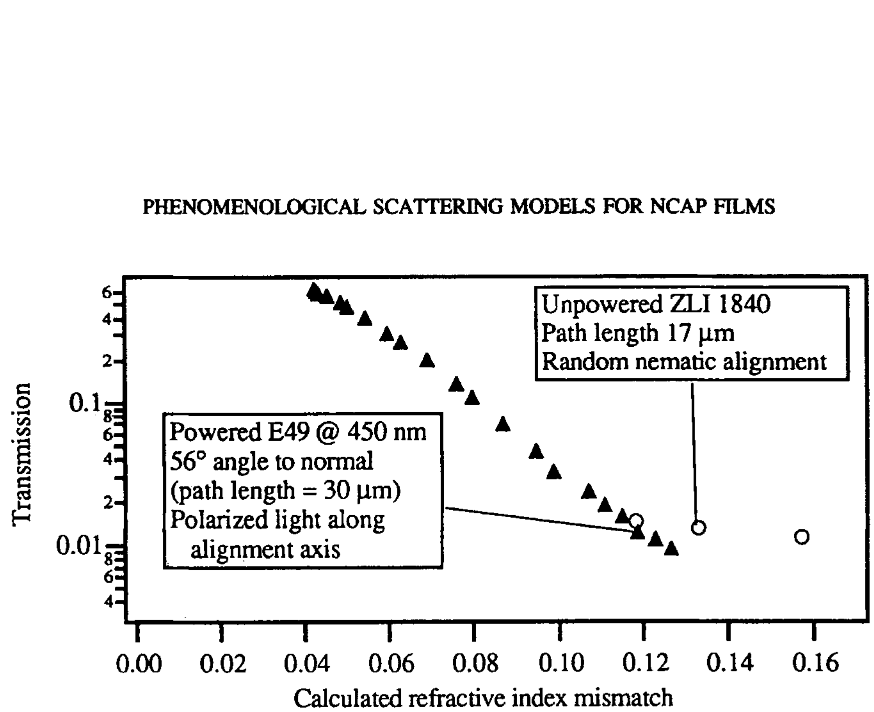

Figure 6. Relative transmission vs. calculated refractive index mismatch for powered E49 @ 450 nm, and unpowered ZLI 1840 @ 650, 550, and 450 nm. Transmission values are corrected for reflection losses but not for path length differences.

If LC/polymer gradients were the only factors inducing scattering in both powered and unpowered films, we would expect the unpowered ZLI 1840 films measured to exhibit only about 1/4 the absorbance (-log[T]) value of the powered E49 film. In fact, the scattering in both sets is similar, which indicates that the dominant scattering mechanisms in the powered and unpowered films are not the same. LC/LC RI gradients provide a mechanism for an enhancement of the scattering cross section for the ZLI 1840 droplets.

To explain the data in Figure 6, we claim that LC/LC correlation provides an important source of RI gradients in the unpowered films described here. While our scaling factor of 4x for the differences in optical path length and nematic alignment differences between films must be viewed with some caution, it appears that in these films LC/LC RI gradients are very important in determining the unpowered scattering properties of these and related films.

Finally, we dismiss the importance of refractive index gradients within droplets as an important source of scattering within these films. This conclusion is based on two sets of experiments. First, the data in Figure 2 shows that scattering of light polarized perpendicular to the alignment direction is weak for $n_{mis} < 0.002$. In these powered films, LC/LC and LC/polymer RI gradients are both minimized. Since the overall scattering is weak, any contribution of the internal RI gradient to the film scattering must be small. We get similar results for films when we align the droplets with mechanical shear, rather than an electric field.[16] Again, light polarized perpendicularly to the alignment direction is scattered only weakly, consistent with internal RI gradients contributing little to film scattering.

Conclusions and prospects

The data presented here shows how films constructed with similar morphologies but different RI values possess high-field scattering properties that can be related to n_{mis}, the RI difference between the droplet and polymer. In powered films, the LC/polymer RI gradient determines the scattering cross section for a droplet. In contrast, we present indirect evidence that indicates that the LC/LC RI gradient is extremely important in determining the scattering cross section in unpowered films. We expect that the studies outlined here will provide a basis for future work probing these phenomenological factors controlling film scattering in these devices.

Acknowledgment

We thank Dr. Ulrich Finkenzeller of E. Merck for providing the wavelength-dependent dispersion data for the nematic mixtures used in this study.

[1]J. L. Fergason, SID Technical Digest (Society for Information Display), **16**, (1986), 68-70.
[2]P.S. Drzaic, J. Appl. Phys., **60**, (1986), 2142-2148.
[3]J. W. Doane, N. A. Vaz, B.-G. Wu, and S. Zumer, Appl. Phys. Lett., **48**, (1986), 269-271.
[4]S. Zumer and J.W. Doane, Phys. Rev. A., **34**, (1986), 3373-3385.
[5]S. Zumer, A. Golemme, and J.W. Doane, J. Opt. Soc. Am. A, **6**, (1989), 403-411.
[6]G.P. Montgomery, Jr., J.L. West, W. Tamura-Lis, J. Appl. Phys. **69**, (1990), 1605-1612.
[7]S. Zumer, Phys. Rev. A., **37**, (1988), 4006-4015.
[8]R.D. Sherman, Phys. Rev. A., **40**, (1989), 1591-1598.
[9]H. Nomura, S. Suzuki, Y. Atarashi, Jap. J. Appl. Phys. **29**, (1990), 522-528.
[10]P. S. Drzaic, Liq. Crystals, **3**, (1988), 1543-1559.
[11]P. S. Drzaic, and A. Muller, Liq. Crystals **5**, (1989), 1467-1475.
[12]B.-G. Wu, J. L. West, and J. W. Doane, J. Appl. Phys., **62**, (1987), 3925-3931.
[13]See, for example, "Geometric and Physical Optics", 2nd Ed., R.S. Longhurst, 1967, Longmans.
[14]See, for example, "Absorption and Scattering of Light by Small Particles", C.F. Bohren and D.R. Huffman, 1983, Wiley and Sons.
[15]G.P. Montgomery, Jr., J. Opt. Soc. Am. B 5 (1988), 774-784.
[16]P.S. Drzaic, unpublished results.